Abstract: In this short review we present our recent results concerning the rotation of atomic Bose-Einstein condensates confined in quadratic or quartic potentials, and give an overview of the field. We first describe the procedure used to set an atomic gas in rotation and briefly discuss the physics of condensates containing a single vortex line. We then address the regime of fast rotation in harmonic traps, where the rotation frequency is close to the trapping frequency. In this limit the Landau Level formalism is well suited to describe the system. The problem of the condensation temperature of a fast rotating gas is discussed, as well as the equilibrium shape of the cloud and the structure of the vortex lattice. Finally we review results obtained with a quadratic + quartic potential, which allows to study a regime where the rotation frequency is equal to or larger than the harmonic trapping frequency.

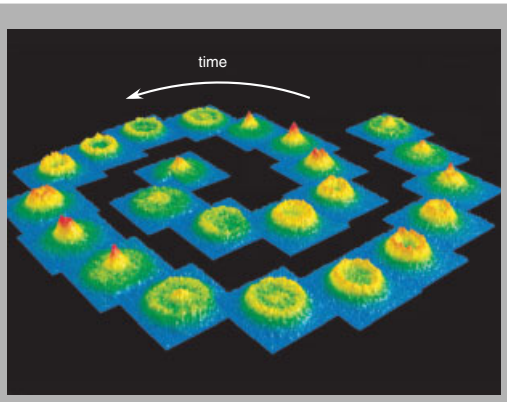

Transverse breathing mode of a fast rotating condensate

Bose-Einstein condensates in fast rotation

S. Stock, B. Battelier, V. Bretin, Z. Hadzibabic, and J. Dalibard *

Laboratoire Kastler Brossel, Unité de Recherche de l'Ecole normale supérieure et de l'Université Pierre et Marie Curie, associée au CNRS, 24 rue Lhomond, 75005 Paris, France

Received: 19 December 2004, Accepted: 23 December 2004
Published online: 18 January 2005

Key words: BEC; vortices; lowest Landau level; rotation; gas

PACS: 03.75.Lm, 32.80.Pj

The possibility to obtain quantum degenerate gases by a combination of laser and evaporative cooling has opened several new lines of research, at the border of atomic, statistical and condensed matter physics (for a review, see e.g. [1–4]). Among them, the rotation of a Bose-Einstein condensate raises many interesting problems with respect to the case of a classical fluid. Since the condensate is described by a macroscopic wave function $\psi(\mathbf{r}) = \sqrt{\rho(\mathbf{r})}e^{i\phi(\mathbf{r})}$, where ρ and ϕ are the spatial density and phase of the fluid, there exist strong constraints on the velocity field of the rotating gas. In a place where the spatial density is not zero, this velocity field is given by $\mathbf{v} = \hbar\boldsymbol{\nabla}\phi/M$ (M is the particle mass), hence $\boldsymbol{\nabla} \times \mathbf{v} = 0$. The circulation of the velocity field is quantized along any close contour on which $\rho \neq 0$, and it is a multiple of h/M. The rotation of the fluid is thus only possible through the nucleation of quantized vortices [5,6], which are singular points (in 2 dimensions) or lines (in 3 dimensions) of vanishing density, and around which the phase ϕ varies by multiples of 2π. Vortices are universal objects which appear in many macroscopic quantum systems, such as superconductors and superfluid liquid helium.

Since the achievement of Bose-Einstein condensation in atomic gases, many experimental and theoretical studies have been devoted to vortices in these systems ([7] and refs. therein). A typical experiment is the following: One starts with a condensate initially at rest, confined in an axisymmetric trap (symmetry axis z), and stirs it by applying an elliptic potential rotating at frequency Ω around z. For very small values of Ω no angular momentum is transferred to the condensate. Just above a critical value Ω_c, a single vortex is nucleated [8]. For a system in thermal equilibrium, the existence of this critical frequency can be viewed as a manifestation of superfluidity: for a slow enough rotation frequency, the stirrer cannot drag the condensate and set it in motion. For stirring frequencies notably larger than Ω_c, the number of vortices in the conden-

* Corresponding author: e-mail: jean.dalibard@lkb.ens.fr

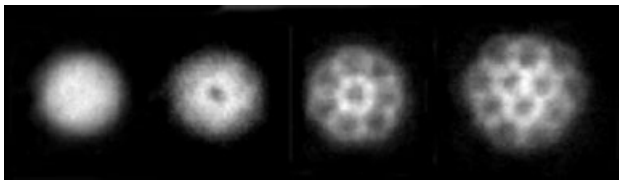

Figure 1 *Quantized vortices.* Absorption images of a stirred Rb Bose-Einstein condensate. The rotation frequency is increasing from left to right (for details see [8])

sate N_v increases, and values up to $N_v = 200$ have been obtained experimentally [9,10].

In the following we will be mostly interested in the large vortex number case, which is achieved by choosing Ω close to the trapping frequency $\omega_\perp$ in the xy plane. Note that in a purely harmonic trap, one must keep Ω below $\omega_\perp$; the centrifugal force otherwise exceeds the trapping force and the gas is destabilized [11]. The main features of the vortex assembly in this large N_v regime are well known. The vortices form a triangular Abrikosov lattice with a surface density $n_v = M\Omega/(\pi\hbar)$ [12]. When $\Omega \to \omega_\perp$, the radius of the gas tends to infinity since the confinement by the trapping potential is nearly balanced by the centrifugal force. Since the surface density of vortices is constant ($\sim M\omega_\perp/(\pi\hbar)$), the number of vortices N_v also increases to arbitrarily large values.

In principle the number of vortices can reach and even go beyond the atom number N. For such a fast rotation, the description of the system by a single macroscopic wave function is expected to fail, and the ground state of the system should be strongly correlated. Up to now this regime has been investigated only theoretically [13–17] and will not be addressed here.

The outline of this short review is as follows. In section 1 we present the mechanism used to set a condensate in rotation. Then in section 2 we briefly review some experiments performed with a single vortex condensate. In section 3, we focus on the fast rotation regime and discuss some important features of this system, such as its condensation temperature and its equilibrium shape. We use the Landau Level approach, which makes a nice connection between this physical problem and that of charged particles in a uniform magnetic field. In section 4 we turn to a configuration that we recently investigated in our laboratory, which consists in superimposing a trapping quartic potential onto the usual quadratic one. This allows us to explore the rotation regime $\Omega > \omega_\perp$, and we review some results obtained for the vortex patterns in this regime. We conclude in section 5 by giving some perspectives of this rapidly evolving field of research.

Note that due to the lack of space this paper does not attempt to be a full review of the work that has been performed on rotating quantum gases but will be subject to the following restrictions: First we will only discuss studies on single component condensates and refer the reader interested in rotating spinor condensates to the recent experiments of the Boulder group ([18] and references therein). Second we will illustrate our discussion using mainly experimental results from our laboratory and only give references to the achievements of other groups. Finally our reference list focuses on papers published after 2001. For a discussion of earlier articles see the detailed review paper by Fetter and Svidzinski [7].

1. Setting a BEC in rotation

In order to nucleate vortices in a condensate, two classes of methods have been used. The first one consists in imprinting on the condensate the phase pattern $e^{i\theta}$ of the desired wave function. It was successfully implemented experimentally by the Boulder group for a two-component condensate [19]. A related scheme, based on the adiabatic inversion of the magnetic field at the center of the magnetic trap, has been used at MIT [20]. The second method, which is used in our group, consists in using a mechanical stirring of the condensate. In order to do this, one can use the potential created by a laser [8,9] or by a magnetic field [21,22]. While the phase-imprinting method is well suited for nucleating a single vortex, the stirring approach seems to be more flexible and allows nucleation of a large number of vortices.

Once the gas is rotating, a third method can be used to increase the angular momentum per particle. It consists in eliminating atoms with an angular momentum smaller than the average, so that the remaining particles rotate at a larger angular speed. This "evaporative spinup" method has been implemented in Boulder [23].

We now present the system that we have been using for rotation experiments in our group. We use rubidium (^{87}Rb) Bose-Einstein condensates produced in a cylindrically symmetric Ioffe-Pritchard trap, with a frequency $\omega_\perp$ in the xy plane and ω_z along the z axis. The magnetic trapping potential thus reads:

$$V_{\mathrm{mag}} = \frac{1}{2}M\omega_\perp^2(x^2+y^2) + \frac{1}{2}M\omega_z^2 z^2\,. \tag{1}$$

Typically $\omega_\perp \sim 10\,\omega_z$ in our experiments so that the equilibrium shape of the condensate is an elongated cigar. For $\omega_z/2\pi \sim 10$ Hz and $N \sim 3\times10^5$ rubidium atoms in the trap, the length of the cigar is 100 μm and its diameter is 10 μm.

We stir the condensate with a laser beam propagating along the z axis. The beam has an anisotropic cross section and its eigenaxes rotate at a frequency Ω. The time-dependent potential created by the laser beam can be written as

$$V_{\mathrm{stir}}(t) = \frac{\epsilon}{2}M\omega_\perp^2\left[(x^2-y^2)\cos(2\Omega t) + \right. \tag{2}$$

$$\left. + 2xy\sin(2\Omega t)\right]\,.$$

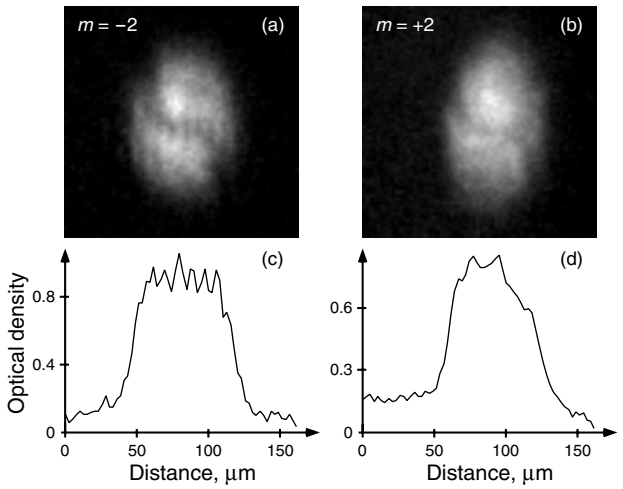

Figure 2 *Kelvin mode of a vortex line*. Transverse images of a Bose-Einstein condensate with a single, positively charged vortex, obtained after excitation of the transverse quadrupole mode $m = -2$ (a) and $m = +2$ (b). Fig. 2a gives an evidence for the Kelvin mode of the vortex line. This mode has an angular momentum $m = -1$, and it is thus excited by the decay of the transverse quadrupole mode $m = -2$ into two "kelvons" (quanta of the Kelvin mode). The two kelvons have the same energy and propagate in opposite directions, which ensures the conservation of linear momentum. By contrast, Fig. 2b shows no oscillation of the vortex line, as expected since the decay of the quadrupole mode $m = +2$ into kelvons ($m = -1$) is forbidden by angular momentum conservation. Figs. 2(c,d) are the corresponding density profiles (for details see [54])

The parameter ϵ is a dimensionless measure of the relative strength of the stirring and the magnetic potentials. In practice we choose $\epsilon \sim 2$–10%.

We apply the stirring potential onto the condensate for a fraction of a second, in order to transfer angular momentum to the gas. The condensate then equilibrates in the cylindrically symmetric potential (1) for ~ 1 second. The trapping magnetic field is then switched off and the gas undergoes a ballistic expansion for a period of ~ 20 ms. Finally, we perform absorption imaging along the rotation axis z. The vortices which have been nucleated in this process appear as density dips in the images, as seen in Fig. 1.

When studying theoretically the problem of a rotating gas, one usually assumes that an arbitrarily small anisotropic potential, rotating at frequency Ω, is added to the main isotropic trapping potential. In presence of this stirring potential, the frame rotating at Ω is the only one in which the state of the system is stationary. The hamiltonian H in this rotating frame is deduced from the hamiltonian in the lab frame $H_{\rm lab}$ by $H = H_{\rm lab} - \Omega L_z$. Experimentally, as we just described, the rotating potential is often switched off for some period before the measurement. Ω then plays the role of the Lagrange multiplier associated with the deposited angular momentum L_z, which is a constant of motion when the system evolves in the axisymmetric potential.

In the following we will mainly focus on the equilibrium properties of the rotating system. We refer the reader interested in the dynamics of vortex nucleation and decay to [24–38].

2. Single vortex physics

For a proper choice of Ω and the equilibration time after stirring, it is possible to nucleate in a reliable way a single vortex in the center of the condensate. Several experimental studies have been performed on such a system. First, the average angular momentum per particle L_z has been measured and found to be of the order of $\hbar$ [39]. This measurement was performed using the relation between L_z and the frequencies of the transverse quadrupole modes of the condensate [40]. Complementary information has been obtained using atom interferometry to measure the phase pattern of the wave function [41,42].

Concerning the vortex line itself, its equilibrium shape has been determined: the line is often curved at the two ends of the cigar [43]. This bending is a symmetry breaking effect, and it can be understood by noticing that a radially centered vortex is favored at the axial center of the cigar, where the density is large, whereas it costs less energy to radially off-center the vortex line at the ends of the cigar, where the density is low [44–49]. Some specific normal modes of the vortex line have also been observed, such as the precession of a single vortex when it is not aligned with the trap axes [50–53], and the Kelvin mode of the vortex line (see Fig. 2) [54–58].

3. Fast rotation in a harmonic potential

We now address the case of a fast rotating gas where the average angular momentum per particle is large compared to $\hbar$, i.e. in which many vortices have been nucleated. We consider that the gas is confined in a purely harmonic potential (1). We first present the Landau level approach to this problem, which is directly connected to the description of the motion of a charged particle in a uniform magnetic field [59–61]. We then address the determination of the critical temperature of the rotating gas, and we compare the result of the semi-classical approach given in [62] with the treatment using the Landau level basis. We then turn to the discussion of the equilibrium shape of the rotating condensate and the structure of the vortex pattern.

3.1. The Landau level approach

In the frame rotating at frequency Ω, the non-interacting, single particle hamiltonian is $H_0 = H_\perp + H_z$ with $H_z = P_z^2/(2M) + M\omega_z^2 z^2/2$ and

$$H_\perp = \frac{P_x^2 + P_y^2}{2M} + \frac{1}{2}M\omega_\perp^2(x^2+y^2) - \Omega L_z = \qquad (3)$$

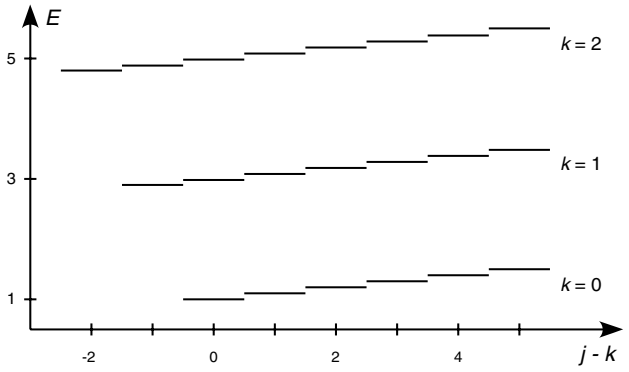

Figure 3 *Landau level structure.* Single particle spectrum for the transverse motion (in the xy plane) for $\Omega = 0.9$. The index k labels the Landau levels. The energy is expressed in units of $\hbar\omega_\perp$

$$= \frac{(\mathbf{P}_\perp - \mathbf{A})^2}{2M} + \frac{1}{2}M(\omega_\perp^2 - \Omega^2)(x^2 + y^2)\,, \qquad (4)$$

where the vector potential is $\mathbf{A} = M\boldsymbol{\Omega} \times \mathbf{r}$. Eq. (4) is formally identical to the hamiltonian of a particle of charge 1 placed in a uniform magnetic field $2M\Omega\hat{\mathbf{z}}$, and confined in a harmonic potential of frequency $\sqrt{\omega_\perp^2 - \Omega^2}$. The Coriolis force, which has the same mathematical structure as the Lorentz force, originates from the vector potential $\mathbf{A}$, whereas the term $-M\Omega^2(x^2 + y^2)/2$ corresponds to the centrifugal potential.

Common eigenstates of H_0 and L_z have single particle energies

$$\frac{E_{j,k,n}}{\hbar} = \omega_\perp + \frac{\omega_z}{2} + j(\omega_\perp - \Omega) + \qquad (5)$$
$$+k(\omega_\perp + \Omega) + n\omega_z$$

and angular momentum $\hbar(j - k)$, where j, k, n are non-negative integers. For Ω close to $\omega_\perp$, the contribution of the transverse motion to these energy levels (terms in j and k) groups in series of states with a given k, corresponding to the well known Landau levels (Fig. 3). The lowest energy states of two adjacent Landau levels are separated by $\hbar(\omega_\perp + \Omega)$, whereas the distance between two adjacent states in a given Landau level is $\hbar(\omega_\perp - \Omega)$. When $\Omega = \omega_\perp$, all states in a given Landau level are degenerate. Physically, this corresponds to the case where the centrifugal potential exactly balances the trapping force in the xy plane, and only the Coriolis force remains. The system is thus invariant under translation, hence the macroscopic degeneracy.

When interactions between particles are taken into account, the Landau levels are no longer eigenstates of the $N-$body hamiltonian. However they are still relevant in the regime of fast rotation. Indeed as $\Omega \to \omega_\perp$, the restoring force in the xy plane becomes very small and the density of the gas drops. The interaction energy per particle is then small compared to the distance $2\hbar\omega_\perp$ between two Landau levels, and the states of interest are essentially those associated with $k = 0$, i.e. the lowest Landau level (LLL) [59–61]. Any function $\psi(x, y)$ of the LLL can be cast in the form:

$$\psi(x, y) = e^{-(x^2+y^2)/2a_\perp^2}\, P(x + iy)\,, \qquad (6)$$

where $a_\perp^2 = \hbar/(m\omega_\perp)$ and $P(u)$ is a polynomial (or other analytic function) of u. When $P(u)$ is a polynomial of degree n, it has n complex zeroes. Each zero is the position of a singly-charged, positive vortex, since the phase of $\psi(\mathbf{r})$ changes by 2π along a closed contour encircling the zero.

3.2. Critical temperature for a rotating gas

The critical temperature for an ideal rotating gas in a harmonic potential has been derived by S. Stringari using a semi-classical approach [62]. Let us briefly outline the reasoning. One starts from the semi-classical relation between the atom number N and the temperature T at the BEC transition:

$$N = \frac{1}{h^3}\int d^3r\, d^3p\, \frac{1}{\exp(H_0(\mathbf{r}, \mathbf{p})/k_BT) - 1}\,, \qquad (7)$$

where we assume that the minimum of the trapping potential is at zero energy, so that we set the chemical potential also equal to zero at the transition point. Using the form (4) of $H_\perp$ and making the change of variables $p'_x = p_x + M\Omega y$, $p'_y = p_y - M\Omega x$, we obtain a new integral. This integral is identical to the one giving the condensation criterion for a gas at rest, confined in a cylindrically symmetric, harmonic potential. The transverse and longitudinal frequencies for this model system are $\sqrt{\omega_\perp^2 - \Omega^2}$ and ω_z, respectively, and we thus get:

$$N = \zeta(3)\left(\frac{k_BT}{\hbar\bar{\omega}}\right)^3\,, \qquad \bar{\omega}^3 = (\omega_\perp^2 - \Omega^2)\omega_z\,, \qquad (8)$$

where $\zeta(x) = \sum_n n^{-x}$ is the Riemann zeta function ($\zeta(3) \simeq 1.202$). This entails that, within the semi-classical approximation, the Coriolis force associated with the vector potential $\mathbf{A}(\mathbf{r})$ has no effect on the critical temperature. This is formally identical to the Bohr – van Leeuven theorem, stating that there is no magnetism at thermal equilibrium in a system of charges described by classical mechanics. The only effect of rotation in (8) is the change of the transverse frequency due to the centrifugal force.

The result (8) can be recovered from the exact one-body spectrum in terms of Landau levels given in (5). Indeed this spectrum is the same as that of a 3D harmonic oscillator with frequencies $\omega_\perp - \Omega$, $\omega_\perp + \Omega$, ω_z, whose geometrical mean is the frequency $\bar{\omega}$, hence the result (8).

We now discuss briefly the validity condition of (8). From the reasoning based on the Landau level structure, we see that k_BT must be large compared to each of the three energies $\hbar(\omega_\perp \pm \Omega)$ and $\hbar\omega_z$. In practice, we have $\omega_\perp \gg \omega_z$ for a cigar-shape trap, so that when $\Omega \sim \omega_\perp$,

the most stringent validity condition for the use of (8) is $k_BT \gg 2\hbar\omega_\perp$. It is not easy to recover this validity condition directly from the use of (8). Indeed one could have naively expected that $k_BT \gg \hbar\sqrt{\omega_\perp^2 - \Omega^2}, \hbar\omega_z$ would be a sufficient condition, which is clearly not the case.

3.3. The equilibrium shape of the rotating condensate

We now suppose that the gas is at zero temperature and review possible approaches for determining its ground state when repulsive interactions are taken into account. As usual in the physics of cold gases, these interactions are assumed to be point-like, and they are characterized by the s-wave scattering length a_s. The ground state $\phi(\mathbf{r})$ of the gas is obtained in the mean-field approximation by minimizing the energy per particle [3,4]

$$E[\phi] = \int \left(\phi^* \left[H_0 \phi \right] + \frac{Ng}{2} |\phi|^4 \right) d^3 r \,, \tag{9}$$

where $g = 4\pi\hbar^2 a_s/M$ and ϕ is normalized to unity.

3.3.1. Rotational hydrodynamics approach

This approach is based on the approximation of diffused vorticity, where the singularities of the velocity field $\mathbf{v}(\mathbf{r})$ and of the atom density $n(\mathbf{r})$ at each vortex core are averaged out. This method is adequate for describing the system at macroscopic distances, larger than the intervortex spacing. From the equations of motion of rotational hydrodynamics [56,63] (see also [65]), one derives the steady state velocity field $\mathbf{v}(\mathbf{r}) = \mathbf{\Omega} \times \mathbf{r}$ and the spatial density $n(\mathbf{r}) = N|\phi(\mathbf{r})|^2$:

$$n(\mathbf{r}) = \tag{10}$$
$$= \frac{1}{g} \max \left(0, \mu - V_{\rm mag}(\mathbf{r}) + \frac{M\Omega^2}{2}(x^2 + y^2) \right) ,$$

where μ is the chemical potential. This density profile is the usual inverted parabola corresponding to the Thomas-Fermi result, for an axisymmetric potential with frequencies $\sqrt{\omega_\perp^2 - \Omega^2}$ in the $xy-$plane and ω_z along the z axis.

The result (10) is valid only if $\mu \gg \hbar\omega_z$. In the opposite regime $\mu \ll \hbar\omega_z$, the z motion is "frozen" to its ground state (a gaussian of extension $a_z = \sqrt{\hbar/(M\omega_z)}$). The relevant wavefunctions can be written as $\phi(\mathbf{r}) = \psi(x,y)e^{-z^2/2a_z^2}$ and one has to minimize

$$E_\perp[\psi] = \int \left(\psi^* \left[H_\perp \psi \right] + \frac{NG}{2} |\psi|^4 \right) d^2 r \,, \tag{11}$$

where $G = g/(\sqrt{2\pi}\, a_z)$. The spatial density in the transverse plane $n(x,y) = N|\psi(x,y)|^2$ is then:

$$n(x,y) = \tag{12}$$
$$= \frac{1}{G} \max \left(0, \mu - \frac{1}{2} M(\omega_\perp^2 - \Omega^2)(x^2 + y^2) \right) ,$$

As for the determination of the critical temperature, only the centrifugal potential is important in this approximation. The Coriolis force plays no role in the global equilibrium shape of the condensate.

3.3.2. Equilibrium shape in the LLL

We now suppose that the interaction strength is small enough so that the ground state of the system is essentially a LLL wave function, corresponding to the quantum number $k = 0$ in Eq. 5 ($\mu \ll 2\hbar\omega_\perp$). We also assume that $\mu \ll \hbar\omega_z$ so that the z motion is "frozen" to its ground state ($n = 0$ in Eq. (5)). The use of LLL wave functions allows to notably simplify the energy functional in Eq. (11). One can indeed prove after some algebra the two equalities:

$$\langle E_{\rm kin} \rangle = \langle E_{\rm ho} \rangle = \frac{\hbar\omega_\perp}{2} + \frac{\omega_\perp}{2} \int \psi^* \left[L_z \psi \right] d^2 r \,, \tag{13}$$

where the kinetic and harmonic oscillator energies are:

$$\langle E_{\rm kin} \rangle = \frac{\hbar^2}{2M} \int |\boldsymbol{\nabla}\psi|^2 d^2 r \,, \tag{14}$$

$$\langle E_{\rm ho} \rangle = \frac{M\omega_\perp^2}{2} \int r^2 |\psi|^2 d^2 r \,.$$

The energy is then given by

$$E[\psi] = \tag{15}$$
$$= \hbar\Omega + \int \left(M\omega_\perp(\omega_\perp - \Omega) r^2 |\psi|^2 + \frac{NG}{2} |\psi|^4 \right) d^2 r \,.$$

We can express the distances and the energies in units of $a_\perp = \sqrt{\hbar/M\omega_\perp}$ and $\hbar\omega_\perp$, respectively. We then find that the minimization depends only on the dimensionless parameter [64]

$$\Lambda = N \frac{MG}{\hbar^2} \frac{\omega_\perp}{\omega_\perp - \Omega} = \sqrt{8\pi} N \frac{a_s}{a_z} \frac{\omega_\perp}{\omega_\perp - \Omega} \,.$$

When $\Lambda < 1$, the interaction term $NG|\psi|^4$ plays a negligible role and the minimizing function is essentially the ground state of the one-body hamiltonian $j = k = n = 0$. For $\Lambda \gg 1$ the minimum energy state is a linear combination of several states corresponding to different quantum numbers j's, and it involves several vortices in the region where the atomic density is significant.

The minimization of (15) within the LLL has recently been discussed in [66,67,64]. Let us briefly sketch the main results. One first defines the coarse-grain average $\bar{n}(x,y)$ of the spatial density $n(x,y) = N|\psi(x,y)|^2$, in order to smooth the rapid variations at the vortex cores. The energy functional (15) can be written in terms of $\bar{n}$ instead of n, provided the interaction parameter G is renormalized

to bG, where $b \simeq 1.16$ is the so-called Abrikosov parameter [68]. This parameter arises from the discreteness of the vortex distribution: since the wave function $\psi(x, y)$ must vanish at the vortex location, the average value of $|\psi|^4$ over the unit cell, hence the interaction energy, is larger than the result obtained if $|\psi|$ was quasi-uniform over the cell. Once this renormalization of G has been performed, the minimization can be performed by letting $\bar{n}$ vary over the whole space of normalisable functions, the only constraint being that $\bar{n}$ varies smoothly over $a_\perp$, which is the characteristic length scale for vortex spacing. One finds that the coarse-grain average of the spatial distribution is the inverted parabola:

$$\bar{n}(x, y) = \tag{16}$$

$$= \frac{1}{bG} \max\left(0, \mu - M\omega_\perp(\omega_\perp - \Omega)(x^2 + y^2)\right) .$$

This result is valid when the chemical potential μ is much smaller than the distance $2\hbar\omega_\perp$ between the LLL and the first excited LL, which amounts to:

$$N\frac{a_s}{a_z} \ll \frac{\omega_\perp}{\omega_\perp - \Omega} .$$

Except for the Abrikosov coefficient b, the two results (12) and (16) nearly coincide in the fast rotation limit, since $\omega_\perp^2 - \Omega^2 \simeq 2\omega_\perp(\omega_\perp - \Omega)$ when $\Omega \sim \omega_\perp$.

The fact that the equilibrium shape of the condensate remains an inverted parabola even when the dynamics is restricted to the LLL has been checked experimentally by the Boulder group [69, 70].

3.3.3. Structure of the vortex pattern

In first approximation the surface density n_v of vortices in a fast rotating condensate is uniform. One can show in this case that the coarse-grain average of the velocity field is equal to the rigid-body rotation result $\mathbf{v}(\mathbf{r}) = \Omega\hat{\mathbf{z}} \times \mathbf{r}$ [12], with $\Omega = \pi\hbar n_v/M$. For rotating BECs, this relation has been checked experimentally at MIT [71]. The vortices form a triangular lattice which is known to minimize the interaction energy $g\int |\psi|^4$ [72].

A closer analysis of the vortex distribution shows that the vortex distribution is distorted on the edges of the condensate [73, 66, 67, 64]. The distortion is particularly clear in the LLL, as it can be seen in Fig. 4 obtained by Aftalion et al. [64], where an example of vortex distribution is given for the particular case $\Lambda = 3000$. This distortion of the vortex lattice is essential to ensure the proper decay of the atomic density given in (16). Indeed an LLL wave function with a uniform vortex lattice always leads to a Gaussian average distribution $\bar{n}(x, y)$ [61], instead of the predicted and observed inverted parabola (16).

Another interesting characteristic of the LLL is that the vortex core is of the same size as the distance between adjacent vortices ($\sim a_\perp$). In this respect the entrance in the LLL for a rotating condensate in a magnetic trap is the equivalent of the field H_{c2} in a type II superconductor [74, 65]. Finally we note that the dynamics of the vortex lattice itself raises many interesting problems. In particular the so-called Tkachenko modes of the lattice have been analyzed theoretically [75, 77–82] and observed experimentally [76].

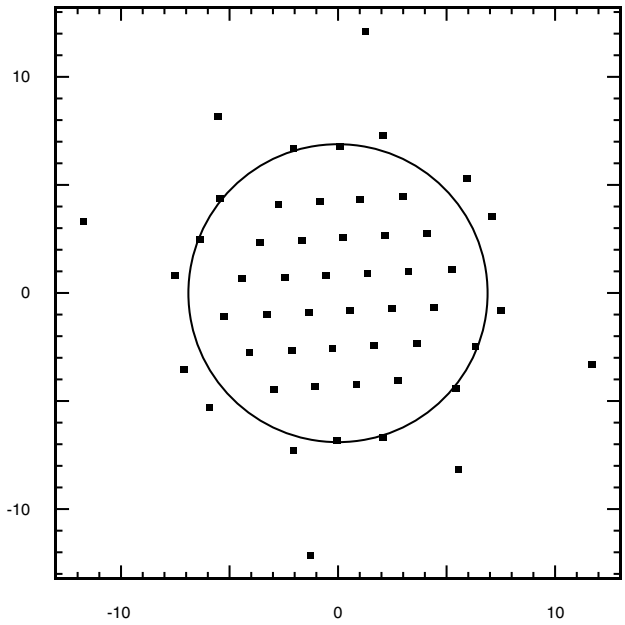

Figure 4 *Vortices in the LLL.* Equilibrium vortex pattern obtained by minimizing the energy within the LLL, for $\Lambda = 3000$ (figure extracted from [64]). The distances are expressed in units of $a_\perp$. The LLL trial wave functions have 52 vortices and the circle represents the border of the Thomas-Fermi distribution (16)

4. Fast rotation in a quadratic+quartic potential

In this section we discuss some results obtained with a quartic potential $\gamma r_\perp^4$ added to the usual harmonic confinement (we set $r_\perp^2 = x^2 + y^2$). This quartic confinement allows to study the regime of rotation where $\Omega > \omega_\perp$. This regime is unreachable otherwise, since the expelling centrifugal potential $-M\Omega_\perp^2 r_\perp^2$ would exceed the trapping potential. The properties of the rotating gas in a quartic potential have recently attracted a lot of theoretical attention [83–90].

4.1. Implementation of a quartic potential

Experimentally, we have created a quartic potential using a far detuned laser beam (wavelength 532 nm), propagating along the axis of the trap [91]. The waist w of the beam

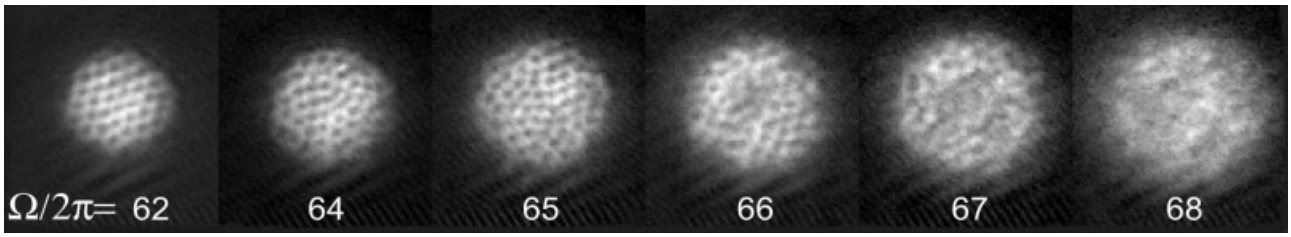

Figure 5 *Vortex pattern in the fast rotation regime.* Pictures of the rubidium condensate rotating in the quadratic+quartic potential, for various stirring frequencies $\Omega/2\pi$. For these data $\omega_\perp/2\pi = 65$ Hz (pictures from [91])

is larger that the condensate radius, so that the potential created by the laser $U_0\ \exp(-2r_\perp^2/w^2)$ can be written as:

$$U(\mathbf{r}) \simeq U_0 - \frac{2U_0}{w^2} r_\perp^2 + \frac{2U_0}{w^4} r_\perp^4 \,. \tag{17}$$

The laser frequency is larger than the atom resonance frequency, so $U_0 > 0$. The second term in (17) leads to a reduction of the transverse trapping frequency $\omega_\perp$ and the third term provides the desired quartic confinement, with $\gamma = 2U_0/w^4$. In our experiments $\gamma = 6.5 \times 10^{-12}$ Jm^{-4}.

The total trapping potential in the xy plane can be written as:

$$V(\mathbf{r}_\perp) = \frac{1}{2} M\omega_\perp^2 r_\perp^2 \left(1 + \tilde{\gamma}\frac{r_\perp^2}{a_\perp^2}\right) , \tag{18}$$

where the dimensionless number $\tilde{\gamma} = 2\hbar\gamma/(M^2\omega_\perp^3)$ characterizes the relative strength of the quartic and the quadratic potentials. For our setup we have $\omega_\perp/2\pi = 65$ Hz and $\tilde{\gamma} \simeq 10^{-3}$. Hence the quartic term is only a small perturbation of the ground state of the one-body hamiltonian. Of course its importance grows when one considers large L_z states, in which the particle is localized further away than $a_\perp$ from the center of the trap.

4.2. Critical temperature

We now determine the critical temperature T_c for a gas rotating in a quadratic+quartic potential. For simplicity we consider the case $\Omega = \omega_\perp$ and we use the semiclassical approximation, which is valid if $k_B T_c \gg \hbar\omega_\perp$. Inserting

$$H_0(\mathbf{r}, \mathbf{p}) = \frac{p^2}{2M} + \frac{1}{2} M\omega_z^2 z^2 + \gamma r_\perp^4 \tag{19}$$

in (7) we obtain

$$N = \zeta(5/2)\frac{\sqrt{\pi}}{4}\frac{M(k_B T_c)^{5/2}}{\sqrt{\gamma}\omega_z} , \tag{20}$$

with $\zeta(5/2) \simeq 1.342$. The experimental results shown here were obtained with $N = 3 \times 10^5$ rubidium atoms. This corresponds to a critical temperature of $T_c = 60$ nK for $\Omega = \omega_\perp$, to be compared with $T_c = 120$ nK for a non-rotating gas.

Our experiments were performed in presence of radio-frequency evaporation, which removes all atoms at a distance $r_\perp$ larger than $x_{\rm ev} = 19\ \mu$m from the center (this corresponds to an angular momentum value $m = x_{\rm ev}^2/a_\perp^2 \sim 200$). For $\Omega = \omega_\perp$ the well depth is thus $U_0 = \gamma x_{\rm ev}^4 \simeq 60$ nK, similar to $k_B T_c$. Since the effective temperature T in evaporative cooling is a small fraction of the well depth (typically $U_0/k_B T \sim$ 5–10), the rotating gas is clearly in the degenerate regime when $\Omega = \omega_\perp$.

4.3. Observed vortex patterns

We show in Fig. 5 the images of the rotating gas as the stirring frequency Ω is increased. For $\Omega < \omega_\perp$, the vortex lattice is clearly visible. However when $\Omega > \omega_\perp$ the visibility of the vortices decreases and nearly vanishes for $\Omega = 1.05\omega_\perp$ ($= 2\pi \times 68$ Hz).

The most plausible explanation of this effect is that the vortex lines are still present, but strongly bent when $\Omega > \omega_\perp$. This bending may occur because of the finite temperature of the gas. A recent theoretical study [88] seems to favor this hypothesis: when looking for the ground state of the system using imaginary time evolution of the Gross-Pitaevskii equation, it was found that much longer imaginary times were required to reach a well ordered vortex lattice for $\Omega > \omega_\perp$ than for $\Omega < \omega_\perp$.

4.4. Transverse monopole mode

The study of the normal modes of a Bose-Einstein condensate generally provides insightful information about the system. In order to gain some understanding of the fast rotation regime, we have studied the transverse monopole (or breathing) mode for various rotation frequencies of the condensate.

For a 2D gas at rest in an isotropic harmonic potential of frequency ω, this mode has a frequency $\omega_{\rm mp} = 2\omega$, which does not depend on the strength of the interactions [92,93]. The state of the condensate at time t can be derived from the state at time 0 by a simple scaling transform. The same result holds for a 3D gas confined in

an axisymmetric, cigar shaped potential [94]. In particular the frequency of the transverse breathing mode is still $\omega_{\rm mp} = 2\omega_\perp$ [95]. For a rotating condensate one could have naively expected that the frequency of the mode is changed to $2\sqrt{\omega_\perp^2 - \Omega^2}$ as a consequence of the centrifugal potential. As shown in [63] this result is not correct and the predicted frequency is still $\omega_{\rm mp} = 2\omega_\perp$ for all rotation frequencies Ω. This is a striking example of the influence of the Coriolis force on the system: even though it affects neither the BEC transition temperature nor the cloud's equilibrium shape at $T = 0$, it has a strong impact on the condensate's normal modes. Note that the result $\omega_{\rm mp} = 2\omega_\perp$ holds for any 2-dimensional gas with contact interactions confined in a harmonic potential [92, 93], so that the monopole mode cannot be used to monitor any phase transition – like that to a strongly correlated state.

We have studied experimentally this mode in the quadratic+quartic potential described above [96]. We have checked that the frequency $\omega_{\rm mp}$ remains at $2\omega_\perp$ for rotation frequencies notably smaller than $\omega_\perp$, for which the quartic term plays no significant role. When the rotation frequency approaches $\omega_\perp$ we measure however a small deviation from this value. This deviation increases with the rotation frequency and reaches $\sim 10\%$ when $\Omega \sim \omega_\perp$. This result is a consequence of the action of the quartic potential and it can be accounted for by a simple analytic model [96]. Due to this deviation the monopole frequency might represent a sensitive tool to monitor the emergence of new quantum phases of the rotating gas.

A remarkable feature of the transverse monopole mode in the region $\Omega \sim \omega_\perp$ is the time evolution of the density profile of the cloud. Instead of being simply a scaling transform as in the pure harmonic case, we observe a phenomenon of entering waves (Fig. 6). This structure can be explained by noticing that for $\Omega \sim \omega_\perp$ several $m = 0$ modes have a frequency close to $\omega_{\rm mp}$ [96], so that beating between them can lead to the observed phenomenon.

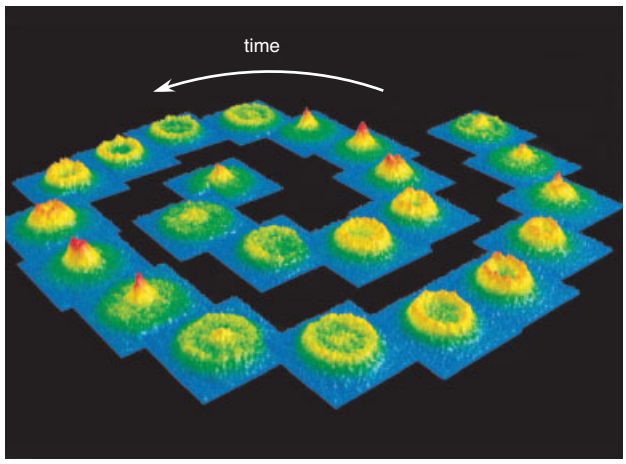

Figure 6 (online color at www.lphys.org) Transverse breathing mode of a condensate rotating at $\Omega = 1.05\omega_\perp$ ($\Omega/2\pi = 68$ Hz). The condensate is confined in the quadratic+quartic potential described in the text. The structure of the mode corresponds to entering waves, instead of a simple scaling transform as in the pure harmonic case. The time interval between two successive pictures is 1 ms

5. Conclusions and perspectives

To conclude, the physics of a rotating Bose gas presents strong analogies with several aspects of condensed matter physics: superconductivity in large magnetic fields, Quantum Hall phenomena, superfluidity and rotating bucket experiments. It has already led to spectacular findings such as the possibility to directly visualize the vortices and to observe their vibration modes such as the Kelvin mode (oscillation of a vortex line) and the Tkachenko mode (oscillation of the vortex lattice). However, important aspects of the problem remain experimentally unexplored. Let us briefly outline three lines of research that seem very promising:

– The possibility to generate quadratic + quartic potential opens the way to the nucleation of stable giant vortices. In a quadratic potential a vortex with a topological charge larger than 1 is unstable, and it can only be observed in a transient way [23,97]. When a quartic potential is present, this instability may disappear and a giant vortex can be stabilized at the center of the trap, possibly surrounded with singly-charged vortices [83–89,74].
– The combination of rotation and optical lattices opens a very interesting class of problems. If a 1D optical lattice is applied along the axis of rotation, one obtains a stack of rotating parallel layers. The structure of vortices in this system remains to be investigated. One can qualitatively expect that the vortex cores in neighboring layers will remain aligned if the tunneling between layers is large enough, whereas they may decorrelate otherwise [98].
– When the rotation speed increases, the number of vortices N_v also increases. When it becomes of the order of the particle number N, one expects that the ground state of the gas will no longer be well described by a mean-field approximation. Instead it becomes a strongly correlated state, with a structure very similar to those appearing in fractional quantum Hall effect [13–17]. In practice these type of states are expected to be observable only for small particle numbers.

With such general lines of research still fully open, the next few years should bring us a lot of novel and fascinating physics.

Acknowledgements We thank Amandine Aftalion, Yvan Castin, Christophe Salomon, and Sandro Stringari for numerous useful discussions. Z.H. acknowledges support from a Chateaubriand grant, and S.S. from the Studienstiftung des deutschen Volkes,

DAAD, and the Research Training Network *Cold Quantum Gases* HPRN-CT-2000-00125. This work is supported by CNRS, Collège de France, Région Ile de France, and DRED.

References

[1] E.A. Cornell and C.E. Wieman, Rev. Mod. Phys. **74**, 875 (2002).
[2] W. Ketterle, Rev. Mod. Phys. **74**, 1131 (2002).
[3] C. Pethick and H. Smith, Bose-Einstein condensation in dilute Bose gases, (Cambridge University Press, 2002).
[4] L. Pitaevskii and S. Stringari, Bose-Einstein condensation, (Clarendon Press, 2003).
[5] E.M. Lifshitz and L.P. Pitaevskii, Statistical Physics, Part 2, chap. III (Butterworth-Heinemann, 1980).
[6] R.J. Donnelly, Quantized Vortices in Helium II, (Cambridge, 1991), Chaps. 4 and 5.
[7] A.L. Fetter and A.A. Svidzinsky, J. Phys. Condens. Matter **13**, R135 (2001).
[8] K.W. Madison, F. Chevy, W. Wohlleben, and J. Dalibard, Phys. Rev. Lett. **84**, 806 (2000).
[9] J.R. Abo-Shaeer, C. Raman, J.M Vogels, and W. Ketterle, Science **292**, 476 (2001).
[10] P. Engels, I. Coddington, P.C. Haljan, and E.A. Cornell, Phys. Rev. Lett. **89**, 100403 (2002).
[11] P. Rosenbusch, D.S. Petrov, S. Sinha, et al., Phys. Rev. Lett. **88**, 250403 (2002).
[12] R.P. Feynman, in: C.J. Gorter (ed.), Progress in Low Temperature Physics, **1**, Chapter 2, (North-Holland, Amsterdam, 1955).
[13] N.R. Cooper, N.K. Wilkin, and J.M.F. Gunn, Phys. Rev. Lett. **87**, 120405 (2001).
[14] B. Paredes, P. Fedichev, J.I. Cirac, and P. Zoller, Phys. Rev. Lett. **87**, 010402 (2001).
[15] J. Sinova, C.B. Hanna, and A.H. MacDonald, Phys. Rev. Lett. **89**, 030403 (2002).
[16] J.W. Reijnders, F.J.M. van Lankvelt, K. Schoutens, and N. Read, Phys. Rev. Lett. **89**, 120401 (2002).
[17] N. Regnault and T. Jolicoeur, Phys. Rev. Lett. **91**, 030402 (2003).
[18] V. Schweikhard, I. Coddington, P. Engels, et al., Phys. Rev. Lett. **93**, 210403 (2004).
[19] M.R. Matthews, B.P. Anderson, P.C. Haljan, et al., Phys. Rev. Lett. **83**, 2498 (1999).
[20] A.E. Leanhardt, A. Görlitz, A.P. Chikkatur, et al., Phys. Rev. Lett. **89**, 190403 (2002).
[21] P.C. Haljan, I. Coddington, P. Engels, and E.A. Cornell, Phys. Rev. Lett. **87**, 210403 (2001).
[22] E. Hodby, G. Hechenblaikner, S.A. Hopkins, et al., Phys. Rev. Lett. **88**, 010405 (2001).
[23] P. Engels, I. Coddington, P.C. Haljan, et al., Phys. Rev. Lett. **90**, 170405 (2003).
[24] B.M. Caradoc-Davies, R.J. Ballagh, and K. Burnett, Phys. Rev. Lett. **83**, 895-898 (1999).
[25] S. Sinha and Y. Castin, Phys. Rev. Lett. **87**, 190402 (2001).
[26] A. Recati, F. Zambelli, and S. Stringari, Phys. Rev. Lett. **86**, 377 (2001).
[27] K.W. Madison, F. Chevy, V. Bretin, and J. Dalibard, Phys. Rev. Lett. **86**, 4443 (2001).
[28] F. Dalfovo and S. Stringari, Phys. Rev. A **63**, 011601 (2001).
[29] M. Linn, M. Niemeyer, and A.L. Fetter, Phys. Rev. A **64**, 023602 (2001).
[30] J.R. Abo-Shaeer, C. Raman, and W. Ketterle, Phys. Rev. Lett. **88**, 070409 (2002).
[31] J.E. Williams, E. Zaremba, B. Jackson, et al., Phys. Rev. Lett. **88**, 070401 (2002).
[32] T.P. Simula, S.M.M. Virtanen, and M.M. Salomaa, Phys. Rev. A **66**, 035601 (2002).
[33] M. Tsubota, K. Kasamatsu, and M. Ueda, Phys. Rev. A **65**, 023603 (2002).
[34] A.A. Penckwitt, R.J. Ballagh, and C.W. Gardiner Phys. Rev. Lett. **89**, 260402 (2002).
[35] K. Kasamatsu, M. Tsubota, and M. Ueda, Phys. Rev. A **67**, 033610 (2003).
[36] E. Lundh, J.-P. Martikainen, and K.-A. Suominen, Phys. Rev. A **67**, 063604 (2003).
[37] C. Lobo, A. Sinatra, and Y. Castin, Phys. Rev. Lett. **92**, 020403 (2004).
[38] R.A. Duine, B.W.A. Leurs, and H.T.C. Stoof, Phys. Rev. A **69**, 053623 (2004).
[39] F. Chevy, K.W. Madison, and J. Dalibard, Phys. Rev. Lett. **85**, 2223 (2000).
[40] F. Zambelli and S. Stringari, Phys. Rev. Lett. **81**, 1754 (1998).
[41] S. Inouye, S. Gupta, T. Rosenband, et al., Phys. Rev. Lett. **87**, 080402 (2001).
[42] F. Chevy, K.W. Madison, V. Bretin, and J. Dalibard, Phys. Rev. A **64**, 031601(R) (2001).
[43] P. Rosenbusch, V. Bretin, and J. Dalibard, Phys. Rev. Lett. **89**, 200403 (2002).
[44] A.A. Svidzinsky and A.L. Fetter, Phys. Rev. A **62**, 063617 (2000).
[45] D.L. Feder, A.A. Svidzinsky, A.L. Fetter, and C.W. Clark, Phys. Rev. Lett. **86**, 564 (2001).
[46] J.J. García-Ripoll and V.M. Pérez-García, Phys. Rev. A **63**, 041603 (2001).
[47] J.J. García-Ripoll and V.M. Pérez-García, Phys. Rev. A **64**, 053611 (2001).
[48] A. Aftalion and T. Riviere, Phys. Rev. A **64**, 043611 (2001).
[49] M. Modugno, L. Pricoupenko, and Y. Castin, Eur. Phys. J. D **22**, 235 (2003).
[50] P.O. Fedichev and G.V. Shlyapnikov, Phys. Rev. A **60**, R1779 (1999).
[51] B.P. Anderson, P.C. Haljan, C.E. Wieman, and E.A. Cornell, Phys. Rev. Lett. **85**, 2857 (2000).
[52] S. Stringari, Phys. Rev. Lett. **86**, 4725 (2001).
[53] E. Hodby, S.A. Hopkins, G. Hechenblaikner, et al., Phys. Rev. Lett. **91**, 090403 (2003).
[54] V. Bretin, P. Rosenbusch, F. Chevy, et al., Phys. Rev. Lett. **90**, 100403 (2003).
[55] T. Mizushima, M. Ichioda, and K. Machida, Phys. Rev. Lett. **90**, 180401 (2003).
[56] F. Chevy and S. Stringari, Phys. Rev. A **68**, 053601 (2003).
[57] R.A. Duine and H.T.C. Stoof, Phys. Rev. Lett. **91**, 150405 (2003).
[58] A.L. Fetter, Phys. Rev. A **69**, 043617 (2004).
[59] S.M. Girvin and T. Jach, Phys. Rev. B **29**, 5617 (1984).
[60] D.A. Butts and D.S. Rokhsar, Nature **397**, 327 (1999).
[61] T.L. Ho, Phys. Rev. Lett. **87**, 060403 (2001).
[62] S. Stringari, Phys. Rev. Lett. **82**, 4371 (1999).

[63] M. Cozzini and S. Stringari, Phys. Rev. A **67**, 041602 (2003).
[64] A. Aftalion, X. Blanc, and J. Dalibard, cond-mat/0410665; to appear in Phys. Rev. A.
[65] G. Baym and C.J. Pethick, Phys. Rev. A, **69** (2004).
[66] G. Watanabe, G. Baym, and C.J. Pethick, Phys. Rev. Lett. **93**, 190401 (2004).
[67] N.R. Cooper, S. Komineas, and N. Read, Phys. Rev. A **70**, 033604 (2004).
[68] W.H. Kleiner, L.M. Roth, and S.H. Autler, Phys. Rev. A **133**, 1226 (1964).
[69] V. Schweikhard, I. Coddington, P. Engels, et al., Phys. Rev. Lett. **92**, 040404 (2004).
[70] I. Coddington, P.C. Haljan, P. Engels, et al., cond-mat/0405240.
[71] C. Raman, J.R. Abo-Shaeer, J.M. Vogels, et al., Phys. Rev. Lett. **87**, 210402 (2001).
[72] Y. Castin and R. Dum, Eur. Phys. J. D **7**, 399 (1999).
[73] D.E. Sheehy and L. Radzihovsky, cond-mat/0402637; D.E. Sheehy and L. Radzihovsky, cond-mat/0406205.
[74] U.R. Fischer and G. Baym, Phys. Rev. Lett. **90**, 140402 (2003).
[75] J.R. Anglin and M. Crescimanno, cond-mat/0210063.
[76] I. Coddington, P. Engels, V. Schweikhard, and E.A. Cornell, Phys. Rev. Lett. **91**, 100402 (2003).
[77] G. Baym, Phys. Rev. Lett. **91**, 110402 (2003).
[78] S. Choi, L.O. Baksmaty, S.J. Woo, and N.P. Bigelow, Phys. Rev. A **68**, 031605 (2003).
[79] T.P. Simula, A.A. Penckwitt, and R.J. Ballagh, Phys. Rev. Lett. **92**, 060401 (2004).
[80] T. Mizushima, Y. Kawaguchi, K. Machida, et al., Phys. Rev. Lett. **92**, 060407 (2004).
[81] S.A. Gifford and G. Baym, cond-mat/0405182.
[82] M. Cozzini, L.P. Pitaevskii, and S. Stringari, Phys. Rev. Lett. **92**, 220401 (2004).
[83] A.L. Fetter, Phys. Rev. A **64**, 063608 (2001).
[84] K. Kasamatsu, M. Tsubota, and M. Ueda, Phys. Rev. A **66**, 053606 (2002).
[85] E. Lundh, Phys. Rev. A **65**, 043604 (2002).
[86] G.M. Kavoulakis and G. Baym, New J. Phys. **5**, 51 (2003).
[87] A.L. Fetter, Phys. Rev. A **68**, 063617 (2003).
[88] A. Aftalion and I. Danaila, Phys. Rev. A **69**, 033608 (2004).
[89] A.D. Jackson, G.M. Kavoulakis, and E. Lundh, Phys. Rev. A **69**, 053619 (2004); see also A.D. Jackson and G.M. Kavoulakis, cond-mat/0311066.
[90] A.L. Fetter, B. Jackson, and S. Stringari, cond-mat/0407119.
[91] V. Bretin, S. Stock, Y. Seurin, and J. Dalibard, Phys. Rev. Lett. **92**, 050403 (2004).
[92] L.P. Pitaevskii and A. Rosch, Phys. Rev. A **55**, R853 (1997).
[93] Yu. Kagan, E.L. Surkov, and G.V. Shlyapnikov, Phys. Rev. A **54**, R1753 (1996).
[94] F. Chevy, V. Bretin, P. Rosenbusch, et al., Phys. Rev. Lett. **88**, 250402 (2002).
[95] S. Stringari, Phys. Rev. Lett. **77**, 2360 (1996).
[96] S. Stock, V. Bretin, F. Chevy, and J. Dalibard, Europhys. Lett. **65**, 594 (2004).
[97] Y. Shin, M. Saba, M. Vengalattore, et al., Phys. Rev. Lett. **93**, 160406 (2004).
[98] J.-P. Martikainen and H.T.C. Stoof, Phys. Rev. Lett. **91**, 240403 (2003); J.-P. Martikainen and H.T.C. Stoof, Phys. Rev. A **69**, 053617 (2004); J.-P. Martikainen and H.T.C. Stoof, Phys. Rev. Lett. **93**, 070402 (2004).